Visualizing Pyroclimatology

Benjamin J. Hatchett[1,2*], T. Todd Lindley[3], John T. Abatzoglou[4], Ansley Baring[5], Alexander Gershunov[6], Kristen Guirguis[6], Robert Munroe[7], Nicholas J. Nauslar[8], Eli Orland[9], Alan M. Rhoades[10], Karen C. Short[11], Rochelle P. Worsnop[12], Grace McLeod[13], Emily M. Wells[1,2*]

[1*]Cooperative Institute for Research in the Atmosphere, Colorado State University, 4000 West Laporte Avenue, Fort Collins, 100190, CO, USA.

[2]Affilate working on a cooperative grant with the NOAA/Global Systems Laboratory, 325 Broadway, Boulder, 80305, CO, USA.

[3]National Weather Service, Norman, 120 David L. Boren Blvd. Suite 2400, Norman, 73072, OK, USA.

[4]Management of Complex Systems, School of Engineering, University of California, Merced, West Laporte Avenue, Merced, 100190, CO, USA.

[5]NOAA/Global Systems Laboratory, 325 Broadway, Boulder, 80305, CO, USA.

[6]Scripps Institution of Oceanography, University of California, San Diego, 8622 Kennel Way, La Jolla, 92037, CA, USA.

[7]National Weather Service, Los Angeles, 520 North Elevar St., Oxnard, 93030, CA, USA.

[8]NOAA/Storm Prediction Center, 3833 Development Ave, Boise, 83705, ID, USA.

[9]NASA Goddard Space Flight Center/University of Maryland, Baltimore County, Mail Code 618, Greenbelt, 20771, MD, USA.

[10]Lawrence Berkeley National Laboratory, 1 Cyclotron Rd., Berkeley, 94720, CA, USA.

[11]Rocky Mountain Research Station, United States Forest Service, 5775 US Highway 10 West, Missoula, 59808, MT, USA.

[12]NOAA/Physical Sciences Laboratory, 325 Broadway, Boulder, 80305, CO, USA.

[13]The Nature Conservancy, 4245 North Fairfax Drive, Suite 100, Arlington, 22203, VA, USA.

*Corresponding author(s). E-mail(s): benjamin.hatchett@gmail.com;

Abstract

Background: Wildland fire activity often demonstrates distinct seasonality adhering to the alignment of climatologically favorable fuels, weather, and ignitions. Improved characterization of conditions that increase fire ignition probabilities, extreme fire behavior, and beneficial fire potential would enhance our understanding of fire regimes and provide insight for future wildland fire management.

Methods: We apply a commonly-utilized tool–the climograph–to visually communicate historical wildland fire activity by demonstrating fire seasonality, interannual variability, and past individual fire events at daily resolution using satellite observations in three distinct case study areas. We apply the analysis to three units of analysis (50 states, 128 pyromes, and 122 National Weather Service County Warning Areas) to evaluate cumulative FRP during calendar year 2026 (through 20 July) and place this year into a pyroclimotological perspective.

Results: Detection counts and cumulative fire radiative power (FRP) in the resulting "pyroclimographs" provide first-order indicators of fire activity seasonality (i.e., wildfires or prescribed burns) and when anomalous activity occurs out-of-season. In coastal Southern California, we show how pyroclimographs vary as the region of interest shifts and how their interpretation can be complemented by including climatological interpretations of additional fire environment data. Pyroclimographs help characterize the fraction of FRP contributed from few or many events, i.e., how many days contribute 50% or 90% of total FRP since satellite observations began. The 1 January–20 July 2026 pyroclimographs indicate widespread record-to-near record satellite-era fire activity by mid-2026 across the United States.

Conclusions: Pyroclimographs may aid identification of environmental factors associated with past fire occurrence or provide understanding of typical timing of smoke impacts and their sources, all of which can be interpreted in the context of evolving real-time conditions and used for longer-term planning. Given the current ubiquity as well as current and projected increase of wildland fire in many regions, we recommend considering pyroclimographs as a visualization tool supporting varied applications where information regarding wildland fire seasonality and characteristics will benefit users.

Keywords: climatology, fire history, fire weather, remote sensing, visualization

1 Introduction

Climographs convey a region's climatic seasonal cycle by displaying the monthly mean temperature range and total precipitation (e.g., Lasantha et al. 2022; Al-Yaari et al. 2023). Many regions also demonstrate a seasonal cycle of fire activity resulting from the annual march of plant phenology–a growing season when fuel accumulates and a dormant season when fuel becomes available for combustion–and the interplay of prolonged and short-term weather conditions. Fire events resulting from natural and human ignitions are linked by climate (i.e., precipitation seasonality and long-term drought) and punctuated by weather, including the evolution of precipitation, temperature, humidity, and winds at hourly-to-weekly timescales.

Visually linking the seasonality of environmental conditions to the cycle of fire danger for situational awareness has literally been in the pocket of firefighters as a 'pocket card' for over 20 years (Schlobohm 2000). The term 'pyroclimograph' arose from the juxtaposition of monthly mean temperature and precipitation with monthly burned area (Swetnam et al. 2011). Sablan et al. (2024) developed similar visualizations of monthly fire activity to show the top 10^{th} and bottom 10^{th} percentiles and mean of a historical record as well as highlight a particular year of interest. Sweeney et al. (2025) generated weekly-timescale visualizations and separated prescribed burns (i.e., pile and broadcast) from wildfires to show the distinct seasonalities of wildland fire types.

However, many wildland fires, especially prescribed burns (Hatchett and Wells 2026) or damaging fast fires (Hantson et al. 2022; Balch et al. 2024) burn only for hours or a few days, rendering aggregation to monthly or even weekly timescales potentially misleading. These short timescales of burn periods may occur during periods of increased fuel receptiveness amidst varied background environmental states, implying a climatological perspective also requires consideration of weather. During briefly intensified fire activity, temporal aggregation limits our interpretation of how anomalous the environmental conditions were compared to climatology. Understanding the conditions leading to increased receptiveness of fuels and the potential for extreme fire behavior may support fire management and community adaptation efforts at annual to decadal timescales as well as characterizing a region's general fire environment. This is important for safely and effectively conducting prescribed burning (Worsnop et al. 2026), a necessary component for achieving wildfire resiliency and restoring ecosystem function in fire-requiring regions. Further, understanding the seasonality of fire activity at sub-monthly scales may inform ideal times to promote campaigns for smoke-ready communities (D'Evelyn et al. 2023; Edgeley and Burnett 2025) and other efforts to support community fire prevention (Hesseln 2018; Abatzoglou et al. 2024), mitigation, and preparedness (Hoekstra et al. 2026).

Over two decades of satellite-based fire detections at subdaily timescales make it possible to produce climatologies of fire activity at daily resolution for a user-defined region. Regions can reflect operational needs or efforts supporting emergency and resilience planning. For example, a region could be jurisdictionally defined, such as a county or National Weather Service (NWS) County Warning Area (CWA). It could also be physically-defined such as a watershed, ecoregion (Omernik and Griffith 2014), mountain range (Snethlage et al. 2022), or pyrome (Short et al. 2020). Ultimately, the goal is to provide a flexible capability for visualizing environmental conditions associated with past fire activity and the timing of varied types of wildland fires at an appropriate scale. Decision support opportunities include operational fire management, prescribed burn planning and alerting, pre-season community messaging for wildfire prevention and preparedness (including smoke readiness), prioritization of long-term adaptation and mitigation efforts for hazard reduction, and research activities to better understand conditions supporting varied fire ignition and behavior patterns.

This brief report provides four examples of the construction and interpretation of pyroclimographs utilizing fire detection data to gain insights about fire activity in three fire-prone landscapes. First, we construct pyroclimographs to illustrate fire activity in Colusa County, California, a region with distinct wildfire and prescribed burning seasonality (Figure 1a–b). Second, we show how pyroclimographs can document the near-real-time progression of a fire season in the U.S. Southern Great Plains (Figure 1c–d). Third, we show how results, particularly seasonality, vary across different geographic delineations in coastal Southern California (Figure 2). Fourth, we demonstrate how a more complete pyroclimograph incorporates ancillary fire environment data (Figure 3). Finally, we use climographs and cumulative FRP results to report that in three of 50 states, seven of 128 pyromes, and seven of 122 CWAs have already experienced a top two ranking in annual cumulative FRP in just over the first half of 2026 (1 January–20 July 2026; Figure 4), highlighting the widespread emergence of potentially novel satellite-era fire regimes during 2026.

2 Data

We used satellite fire detections from the 1 km horizontal resolution Moderate Resolution Imaging Spectroradiometer (MODIS) onboard the Terra and Aqua spacecraft (Giglio et al. 2016). Fire detections are processed by NASA to create the MODIS active fire product (MCD14DL) that was acquired from the NASA Fire Information for Resource Management System (https://firms.modaps.eosdis.nasa.gov/) for the period spanning 1 January 2001 to 7 July 2026. MODIS overflights occur at approximately 1030 and 2230 (Terra) and 1330 and 0130 (Aqua) local time, though in recent years some drift has occurred leading to later overflight timing by several hours. County and state shapefiles were acquired from the U.S. Census Bureau (https://www2.census.gov/geo/tiger/TIGER2025/). Shapefiles for the NWS CWAs were acquired from the NWS County Warning Boundary Area Dataset (https://www.weather.gov/gis/CWABounds). The Southern California Mountains/Northern Baja pyrome was extracted from (Short et al. 2020). Environmental Protection Agency (EPA) Level 3 ecoregions were acquired from the EPA's website (https://www.epa.gov/eco-research/level-iii-and-iv-ecoregions-continental-united-states). Last, we used a boundary delineating the Santa Monica Mountains, a subset of the Transverse Ranges and excluding the Palos Verdes Hills, from the Global Mountain Biodiversity Assessment Mountain Inventory version 2.0 (Snethlage et al. 2022,?).

For our fourth pyroclimograph example (Figure 3), we used the energy release component spanning 1979–2025 from the daily, gridded $\sim$4 km horizontal resolution gridMET product (Abatzoglou 2013) as a measure of fire danger. To account for factors that impact fire ignition and spread, we used hourly observations of 2-m relative humidity and 20 ft ($\sim$6-m) wind speed from the Malibu Hills, California Remote Automatic Weather Station (RAWS; acquired from the Western Regional Climate Center at: https://raws.dri.edu) for the station's period-of-record (January 1995–February 2026).

3 Methods

Analysis of fire detection latitude, longitude, fire radiative power (FRP), and time of detection, as well as other fire environment data, was performed using Matlab (The MathWorks Inc. 2024). Desiring maximum detectability, we did not omit detections based on confidence values, which may include anomalous detections due to industry or sun glint. For each calendar day across all years, the total number of detections are counted and reported by a bar chart (Figures 1b,d); specific years of interest can be plotted separately. Similarly, cumulative FRP across each calendar day in the period-of-record is calculated to show seasonality of fire activity (right hand y-axis of Figures 1b and d). Lastly, we calculate the total FRP over the period of record and then sort the daily FRP entries in descending order to determine the number of days that it took to reach the 50%, 75%, and 90% of the total FPR (text beneath Figures 1b,d). While 1 January was selected as the starting point, the visualization can be oriented to meet user needs based on the realized seasonal trends in regional fire activity.

To show the seasonality of fire danger in the Santa Monica Mountains example (Figure 3), gridMET-based estimates of energy release component (ERC) were extracted for a box encompassing the region (Figure 3b). The 3^{rd}, 5^{th}, 20^{th}, 50^{th}, 80^{th}, and 97^{th} percentiles were calculated between 1979–2025 at a daily scale (plotted with 5 day running mean to smooth the data). The 3^{rd}, 50^{th}, and 97^{th} percentiles were calculated across all days.

Fire weather hours were estimated using the available summed daily number of hours between 1995–2024 meeting either set of criteria for a Red Flag Warning at the NWS Fire Weather Zones (FWZ) 369 and 370 (California Annual Operating Plan 2025): 1) relative humidity $\leq$ 10% with sustained wind speed $\geq 6.7\ m\ s^{-1}$ ($\geq 15\ miles\ hr^{-1}$) or gusts $\geq 11.2\ m\ s^{-1}$ ($\geq 25\ miles\ hr^{-1}$) or 2) relative humidity $\leq$ 15% with sustained wind speed $\geq 11.2\ m\ s^{-1}$ ($\geq 25\ miles\ hr^{-1}$) or gusts $\geq 15.6\ m\ s^{-1}$ ($\geq 35\ miles\ hr^{-1}$). If these conditions are sustained for $> 6hr$ with critically dry fuels, a Red Flag Warning may be issued. Under certain extreme conditions, forecasters will coordinate with fire agencies to relax constraints for Red Flag Warning issuance.

To provide a pyroclimatological perspective on the current (2026) calendar year through present (1 January–20 July), cumulative FRP was summed for each year between 1 January and 31 December 2001–2025 and for the period spanning 1 January–20 July 2026 for each CWA, pyrome, and state. Values were sorted in descending order and the position of 2026 in the rankings identified.

4 Results

4.1 Pyroclimographs: A Simple Interpretation and Application

Colusa County, CA–an agricultural community–demonstrates three distinct burn seasons as evidenced by small increases in annual accumulations of FRP during late winter to early spring (mid-January–April), a more rapid increase during the extended summer (late June–September), and a shift back to gradual but annually consistent increases during fall (October–November; Figure 1a). Examining a county level count of burn permit data produced by Worsnop et al. (2026) and wildfire history data hosted by CAL FIRE (https://www.fire.ca.gov/what-we-do/fire-resource-assessment-program; not shown), the consistent daily detections (Figure 1b) with lower FRP indicate the seasonal nature of planned agricultural burning and prescribed burning of wildlands during spring and fall, while more brief instances of higher FRP indicate named summer wildfire incidents (e.g., 2012, 2018, and 2024). Incorporating additional agency (or other) records of prescribed burns versus wildfire events is recommended to differentiate the seasonality of fire types.

Wildfire and prescribed fire occur in the U.S. Southern Great Plains throughout the year, though a peak in fire activity occurs in March following the dry winter season and terminates with the onset of the spring convective season in April leading to the green up of herbaceous and grass fuels (Figure 1c–d). As fire detection data is made publicly available on the order of hours after a satellite overflight, pyroclimographs can be used to track the progression of a fire season in near-real-time. With persistent drought and heavy fine fuel loading priming the fire environment, a dry and windy spring initiated the 2026 wildfire season approximately two weeks early (red line in Figure 1c). Because of overlapping seasonality between planned and unplanned ignitions in the OUN-AMA region during late winter into spring (as well as much of the Southern Great Plains), it is difficult to separate out ignition type. However, in the late summer through early winter, it is more likely that planned ignitions will drive the signal, as evidenced by colored notable fire years composing a smaller fraction of daily fire detections (Figure 1d). While the annual cumulative curves (Figures 1a and 1c) allow the comparison of years against one another–for example, to identify early onset of fire activity–for the remainder of the manuscript, we focus on the detection bar charts (Figure 1b and 1d).

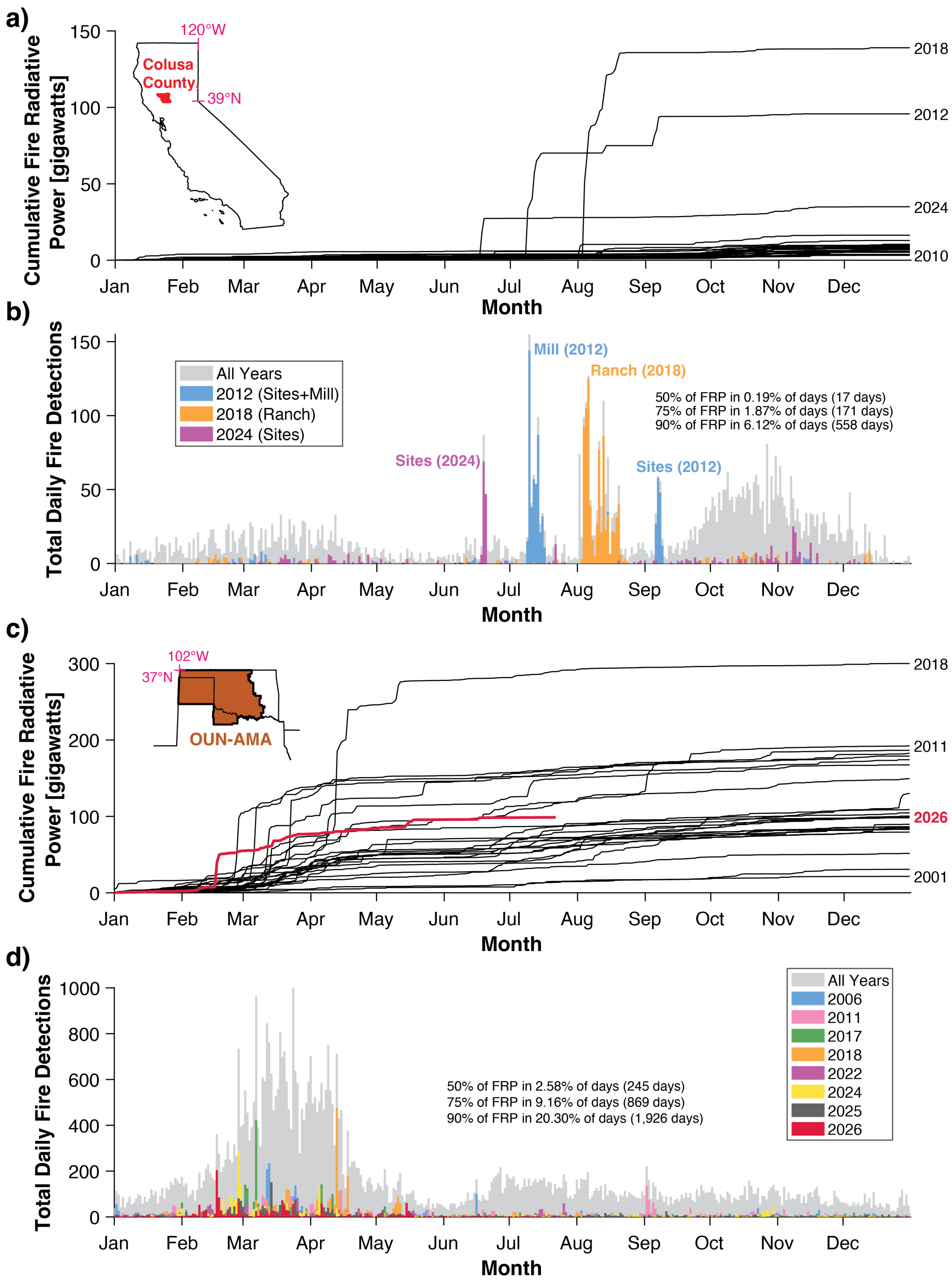

Fig. 1 (a) Pyroclimograph showing daily cumulative fire radiative power for each calendar year (2001–2025; highest three and lowest year labeled) for Colusa County, California. (b) Period-of-record total daily fire detections across years (gray bars). Contributions from notable fires are colored. (c–d) As in (a–b) but for the Norman, Oklahoma (OUN) and Amarillo, Texas (AMA) NWS CWAs (2026 shown in bold red).

4.2 Variability across coastal Southern California

Coastal Southern California is a densely populated, fire-prone but ignition-limited landscape with extraordinary exposure of values-at-risk to wildland fire. Natural ignitions are rare but human ignitions are common (Keeley and Syphard 2019)). Here, we explore how pyroclimographs contribute to fire history interpretation across different domains within the region. The Southern California Mountains/Northern Baja pyrome (largest scale) spans interior Santa Barbara County to San Diego County (Figure 2a). This area experiences its largest and most destructive wildfires between May and early January though the consistent but few detections, with lower FRP, during the cool season indicate potential cool season prescribed burning. Two Environmental Protection Agency Level 3 Ecoregions comprise the pyrome. In the mid-to-higher elevation, conifer-dominated Southern California Mountains ecoregion, fire season typically spans June to mid-October but can include anomalous dry downslope Santa Ana wind-driven fire events such as the late October firestorms in 2003 and 2007 as well as the December 2017 Thomas Fire and January 2025 Eaton Fires (Figure 2b). The lower elevation, chaparral and coast sage and chaparral-dominated Southern California Coast/Northern Baja ecoregion has fewer fires in the summer (one exception being the 2018 Holy Fire), owing to cool and moist marine layer influences, but also includes many destructive coastal fires such as the November 2018 Woolsey Fire and January Palisades 2025 (Figure 2c). Wildfires are most common in late fall and into winter if Santa Ana winds begin before season-ending cool season precipitation occurs. The NWS Los Angeles CWA (Figure 2d) includes more interior dry regions (such as further north where the 2025 Madre and Gifford Fires occurred) and elevated terrain susceptible to human and lightning ignitions. The hotter and drier conditions yield a longer overall fire season from May through early January with a notable peak in activity between July and September.

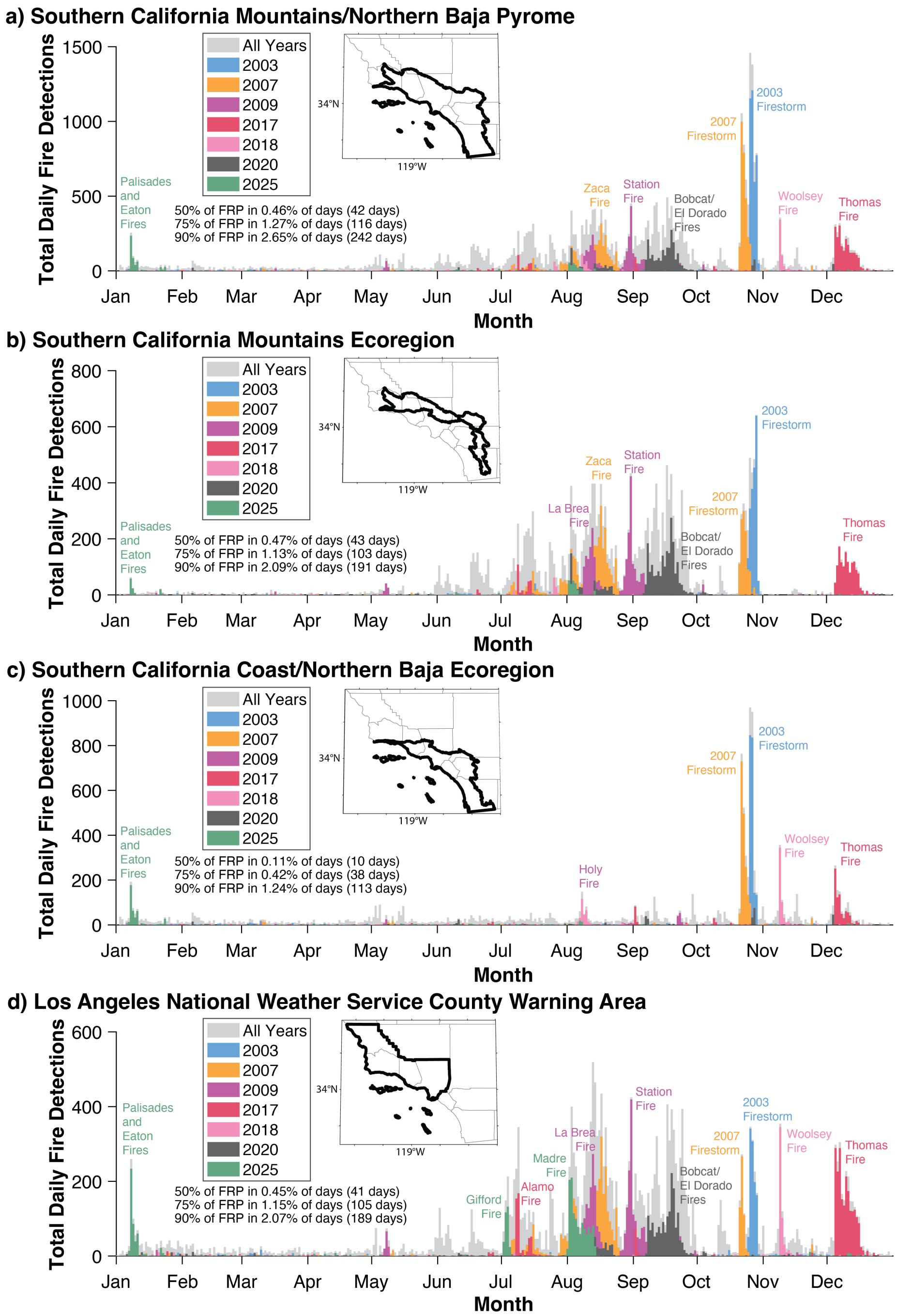

Fig. 2 Figure 2: Pyroclimographs for (a) the Southern California Mountains/Northern Baja pyrome, (b) the EPA Level 3 Southern California mountain ecoregion, (c) the EPA Level 3 Southern California/Northern Baja Coast ecoregion, and (d) the Los Angeles CWA.

4.3 Towards a more complete pyroclimograph

Our motivation to extend the monthly-scale pyroclimograph proposed by Swetnam et al. (2011) is to provide a more complete picture of fire activity and the fire environment at daily timescales. This information can then be included in a format similar to classic pocket card style (Schlobohm 2000) where a satellite-derived daily fire history, ERCs, and BI are shown together. As a demonstration, the Santa Monica Mountains of Ventura and Los Angeles counties represent an ideal location to demonstrate how fire weather deviates from climatological conditions. Here, strong winds and low relative humidity conditions associated with occasional offshore, downslope Santa Ana winds–especially when winds occur before season-ending rainfall (Cayan et al. 2022; Guirguis et al. 2025)–produce extreme fire behavior, with 10 days during the 2001-2025 period contributing 90% of total FRP (Figure 3a). The number of days contributing to a given percentage of total FRP increases as the domain grows larger (Figure 2–3). However, this calculation intends to indicate whether a relatively smaller number of days (10 days here, or 145–242 days in the larger coastal Southern California regions (Figure 2)) or a relatively larger number of days (1,926 days in the OUN–AMA region; Figure 1d) contribute to various fractions of total FRP to provide a simple metric of the frequency and intensity of fire in a region. The Santa Monica Mountains of Ventura and Los Angeles counties represent an ideal location to demonstrate how fire weather deviates from climatological mean conditions. Here, strong winds and low relative humidity associated with occasional offshore, downslope Santa Ana winds–especially when Santa Ana winds occur before fire season-ending rainfall (Cayan et al. 2022; Guirguis et al. 2025)–produce extreme fire behavior, with 10 days contributing 90% of total FRP (Figure 3a). The number of days contributing to a given percentage of total FRP increases as the domain grows larger (Figure 2–3). However, this calculation intends to indicate whether a relatively small number of days (10 days in the Santa Monicas, or 145–242 days in the larger coastal Southern California regions; Figure 2) or a large number of days (1,906 days in the OUN–AMA region; Figure 1d) contribute to various fractions of total FRP to provide a simple metric of the frequency and intensity of fire in a region.

Merging the fire detection climatologies (Figure 3a) with an ERC climatology extends and modernizes the original pocket card (Schlobohm 2000) by including the full fire climatology for comparison with ERC percentiles calculated for days of the year and across the year (Figure 3b). The seasonal cycle of ERC indicates a peak during fall and a minima during spring. The largest range in values occurs in winter and smallest range during summer. The timing and magnitude of these ranges results from the Mediterranean climate and proximity to summer marine influences. Plotting the range-mean ERC on the ignition dates of recent Santa Monica fires (and two nearby high-impact fires, the 2017 Thomas Fire and 2024 Mountain Fire) show that most fire activity occurs in late fall through early winter, the exception being the 2013 Springs Fire that occurred during a spring wind event coinciding with moderate drought conditions per the U.S. Drought Monitor (Svoboda et al. 2002). These fires all ignited on days with above normal ERCs but none exceeded the 97^{th} percentile and many were below the annual 90^{th} percentile.

Until now, pyroclimographs have focused on the ignition component of the fire environment. Inclusion of wind, and particularly wind associated with low relative humidity, incorporates the spread component. Using the two sets of relative humidity and wind criteria for Red Flag Warnings but omitting the wind duration constraint, fire weather hours are relatively rare from May–September before reaching peak frequency during October–November (Figure 3c). They decline through the winter before a secondary peak between March–April, albeit typically when live fuel moisture is high (Guirguis et al. 2025). Just as the ERC climatology highlighted the marine stratus season, fire weather hours highlights two critical fire weather patterns affecting the Santa Monicas: the fall–winter Santa Ana season, followed by a signal of late spring Sundowner Winds that typically affect the Santa Ynez Mountains to the northwest but can also influence the Santa Monicas (Hatchett et al. 2018).

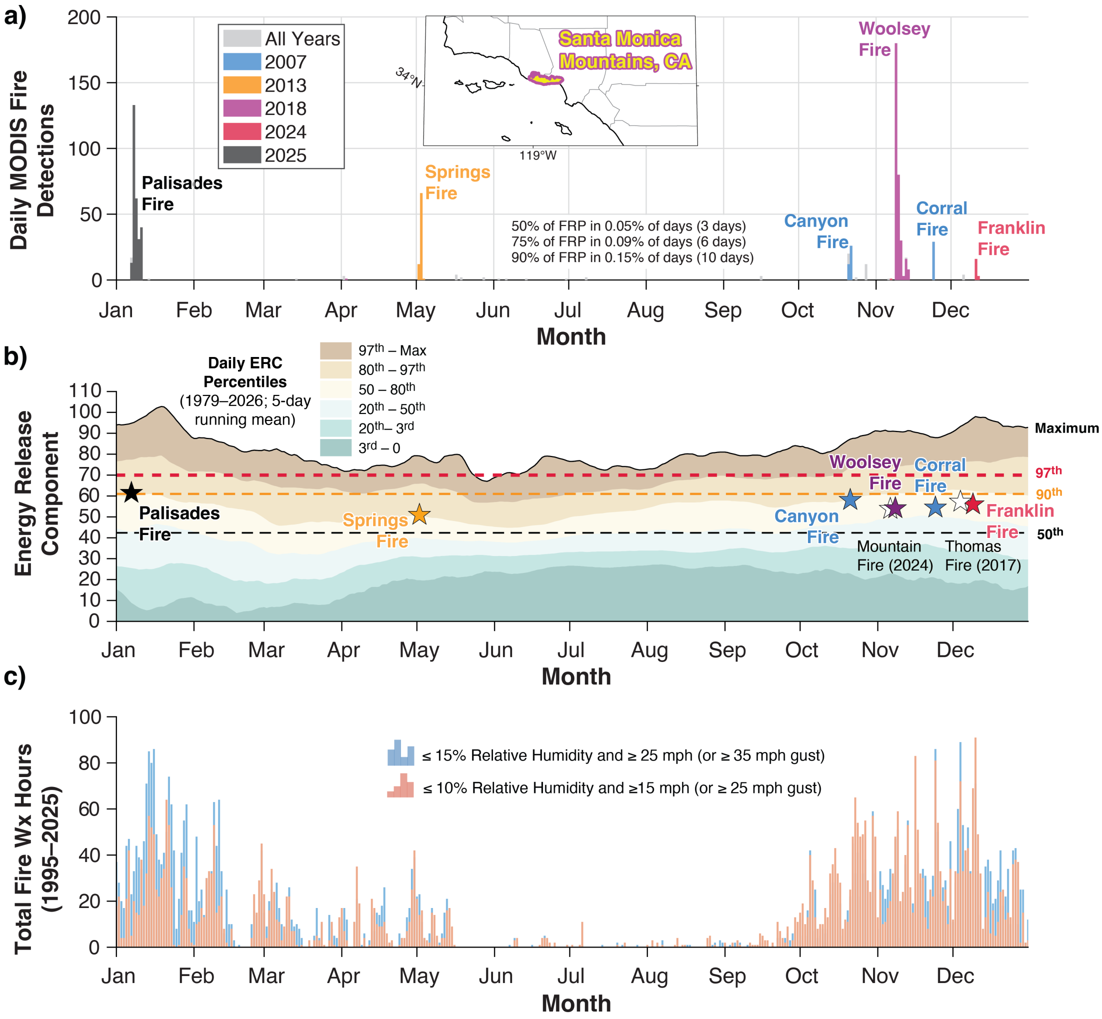

Fig. 3 Pyroclimograph showing period-of-record total daily fire detections (gray bars; left y-axis) for the Santa Monica Mountains of southern California (inset map). Contributions from notable named fires are colored by year. (b) Energy release component daily climatology with shaded regions representing percentile bins. Horizontal dashed lines represent all-time percentiles. For reference, the actual ERCs on the day of ignition for notable fires are provided; two other nearby damaging fires, the 2017 Thomas Fire and the 2024 Mountain Fire are also shown for reference. (c) Total fire daily weather hours spanning January 1995–February 2026 calculated using two sets of wind speed and relative humidity criteria for NWS LOX Red Flag Warnings at the Malibu Hills RAWS.

4.4 A pyroclimatological perspective of the progression of the 2026 calendar year

Pyroclimographs produced at the NWS CWA, pyrome, and state level indicate widespread elevated fire activity in 2026 from 1 January through the time of writing

(20 July). To summarize the 2026 fire year thus far, Figure 4 demonstrates the ranking of cumulative FRP for 2026 compared to the period-of-record of MODIS satellite observations for each of the three geographic delineations. We note 2001–2025 are composed of complete years. Regardless of spatial domain selected, multiple locations across the U.S. are experiencing the most active to second-most active fire years in terms of total FRP and include: seven of 122 NWS CWAs with 12 in the top six years (Figure 4a), seven of 128 pyromes with 17 in the top six (Figure 4b), and three of 50 states with five in the top six (Figure 4c).

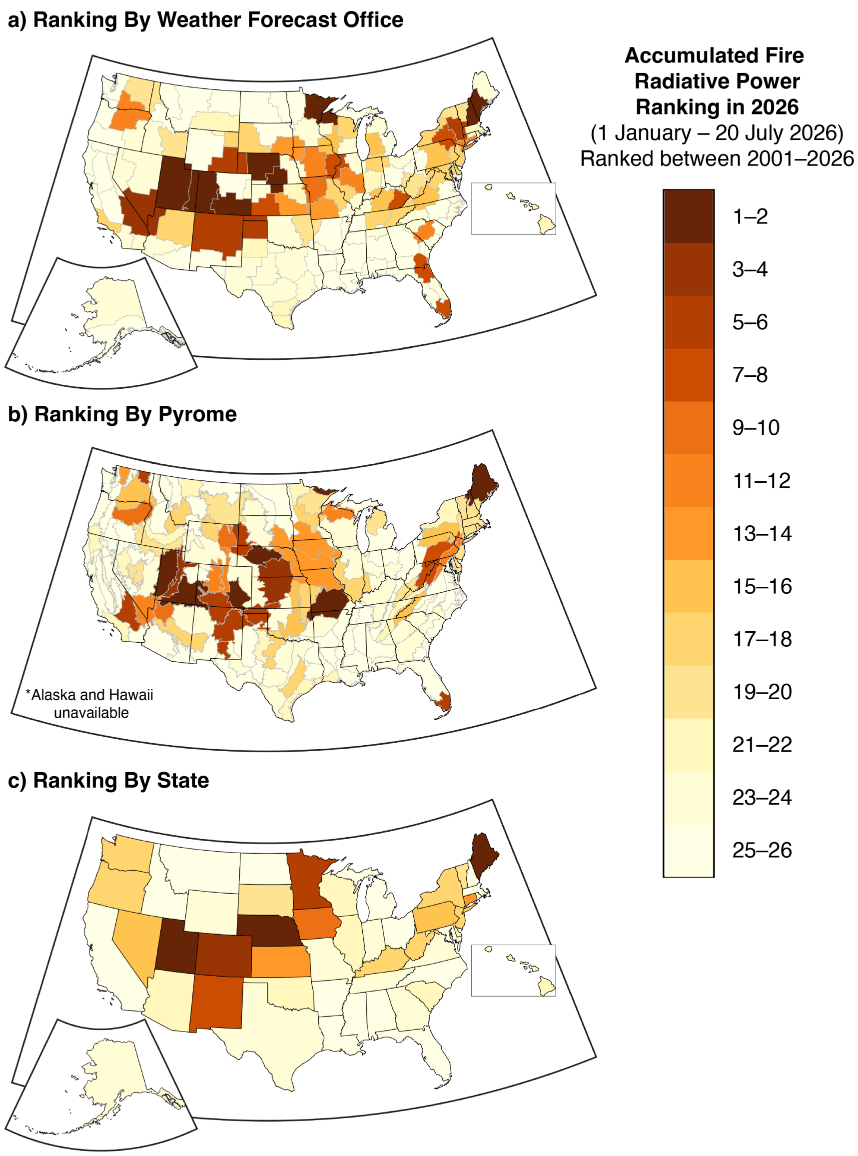

Fig. 4 Ranking of cumulative fire radiative power observed between 1 January – 20 July 2026 against 2001–2025 by (a) NWS CWA, (b) pyrome, and (c) state. The 2026 values are compared against cumulative fire radiative power during complete years (2001–2025).

5 Discussion

Daily-scale pyroclimographs using satellite data provide a more temporally granular and spatially explicit perspective than historical fire perimeters that offer only singular dates of discovery and containment (Swetnam et al. 2011) or monthly aggregations of satellite data (Giglio et al. 2009; Sablan et al. 2024). They also reveal potential prescribed burn seasonality, assuming burning occurred during satellite overflight, through the interpretation of more frequent, low FRP detections. However, integration of authoritative records of prescribed burning and wildfire are necessary to ensure correct interpretations (Sweeney et al. 2025). Assuming a correct interpretation, pyroclimographs can serve as a training tool to understand a region's satellite-era fire history, identify ideal prescribed burning timing, extract information to examine similarities and differences across regions such as fuels-driven versus wind-driven fire location and timing, and as a tool to document and contextualize the evolution of a fire season in terms of how observed fire weather deviated from normal conditions. While we focused on satellite-era fire history, longer records of fire history could be incorporated to increase the comprehensive nature of the pyroclimograph.

The 2026 ranking exercise begets the question: Is 2026, at least thus far, actually anomalous in the regions identified as ranking above all or most other years? Like all fire metrics, FRP is but one method to quantify activity, just like total burned area, area burned at high severity, or number of fires. Beyond implying the presence of fire of varying intensities across an area at the time of satellite overflight, an additional benefit of FRP compared to other metrics is its use as a first-order input to smoke transport models (Ahmadov et al. 2017). This adds additional value to it as a metric indicating a greater likelihood of local, regional, and downstream air quality impacts on health and economic activity when anomalous FRP occurs, making it potentially a more integrated, albeit still singular, metric of fire activity. Take the example of Georgia, which showed up as notable only in the CWA rankings (Figure 4a), experienced the greatest number of structures destroyed in a single fire in its history (110) during the 2026 Highway 82 Fire (Carney 2026). Conversely, all three delineations indicate Utah, Nebraska, and Maine are experiencing their most-to-second-most active fire year in the satellite record, with Colorado and Minnesota in the top four years (Figure 4) despite having much of the fire season remaining.

Beyond merely counting, a benefit of the ranking approach in tandem with using pyroclimographs to understand how a year played out in terms of timing, magnitude, and duration, is a way to identify locations that have not recently experienced notable fire activity. This allows for potential reporting and training activities; for example, what went well and what could be improved at the weather forecast office or state level and what kinds of fire behavior and fire effects occurred at the pyrome level. By combining with other metrics, cumulative FRP rankings could help verify the skill of the Predictive Services outlooks for significant fires (https://www.nifc.gov/nicc/predictive-services/outlooks).

A limitation of our approach is that it visualizes a minimum amount of fire activity: satellites may not capture all pixels burning at all times as wildland fire progresses across the landscape and cannot capture fires that do not produce a detectable heat signature. False positives due to industry or sun glint may cause some overestimation of counts and require additional investigation. An upcoming challenge for data continuity will be to merge MODIS and the Visible Infrared Imaging Radiometer Suite (VIIRS) detection climatologies as the MODIS mission approaches decommissioning and VIIRS becomes a primary fire detection data source. In addition to merging VIIRS into the MODIS record of fire detections and FRP, other existing satellite missions such the 5 minute temporal resolution Geostationary Operational Environmental Satellite Advanced Baseline Imager as well as newly-launched fire detection platforms (e.g., FireSat; https://sites.research.google/gr/wildfires/firesat/) could be similarly integrated with MODIS and VIIRS to create more robust satellite-era fire histories. By increasing the temporal resolution of fire detection through multiple platforms, more precise estimates of environmental conditions at the time of detection can be achieved in addition to estimates of the rate of spread. This will enable verification of forecast weather, fire spread, and fuels conditions and also may facilitate the interpretation of fire effects based on fire intensity, residence time, and environmental conditions.

Reporting climatological mean conditions likely underestimates the potential for fire activity, which may only require several hours to yield favorable conditions for ignition and extreme fire behavior that presents resistance to control. It also prevents clear identification of the frequency, timing, magnitude, and duration of anomalous conditions favoring wildland fire. Fires often occur in regions characterized by additional variability of environmental conditions across timescales including: intraseasonal (winter rain versus mid-winter dry spells followed by dry and windy Santa Anas), interseasonal (fall and winter Santa Ana events versus summer drought or convective storms), and interannual timescales (wet years interspersed with drought years). Thus, the use of ERCs and fire weather hours only estimates the first-order potential for fire ignition and spread in southern California. Identifying the specific conditions associated with burning will aid in the identification of the atmospheric processes driving them, improving their predictability and thus community preparation. Subsequent iterations of pyroclimographs will include local conditions extracted on the day (or at overflight time if possible) of burning to better assess their role during rapid fire spread or high FRP events and how the fire environment influences burn severity (Orland et al. 2025).

6 Closing Remarks

We revisited the concept of pyroclimographs as simple visualizations leveraging satellite fire detections to demonstrate a facet of pyrogeography: the "where of fire when" to understand "the why of fire." Providing a daily perspective of wildland fire activity, pyroclimographs contextualize a region's satellite-era fire history and support the interpretation of past fire events, especially when complemented with fire environment data. With no additional information, a pyroclimograph indicates when fire activity has not (yet) been observed, when fire activity may be common but less with lower FRP (potential prescribed burning) versus infrequent but higher FRP (potential wildfire). By including fire environment-related data and its variability, a picture emerges of why certain seasons typically do or do not have increased fire activity and why anomalous events occurred. The simplicity of these visualizations is intentional; it is our aim that they can be used not just for scientific or tracking purposes but also for educational and training purposes (e.g., when to expect smoke of varying origins for smoke-readiness, when to begin messaging fire prevention and mitigation ahead of fire season, and a way to reflect back on events using an after-action review approach) for anyone willing to interpret a time series for the appropriate domain.

Declarations

- Disclaimer The statements, findings, conclusions, and recommendations are those of the authors and do not reflect the views of NOAA, the U.S. Department of Commerce, the USFS, NASA, or the U.S. Department of Energy.

- Funding Benjamin Hatchett was supported by a NOAA cooperative agreement for the Cooperative Institute for Research in the Atmosphere (NA24OARX432C0007), the Bipartisan Infrastructure Law (BIL) Provision 5, Fire 2 (NA23OAR40504161), the Disaster Relief Supplemental Appropriations Act (NA23OAR4050133D). Alan Rhoades was funded by the Office of Science, Office of Biological and Environmental Research of the U.S. Department of Energy Regional and Global Model Analysis (RGMA) and MultiSector Dynamics (MSD) Program Areas "the Calibrated and Systematic Characterization, Attribution and Detection of Extremes (CASCADE)" Science Focus Area (DE-AC02-05CH11231) and the "An Integrated Evaluation of the Simulated Hydroclimate System of the Continental US" (HyperFACETS) project (DE-SC0016605).

- Data availability Processed MODIS data and pyroclimographs for each WFO, state, and pyrome are being uploaded to a Zenodo repository (available at time of submission for reviewers).
- Code availability Code will be made publicly available on github upon acceptance.

References

Abatzoglou, J.T. 2013. Development of gridded surface meteorological data for ecological applications and modelling. *International Journal of Climatology 33*(1): 121–131. https://doi.org/https://doi.org/10.1002/joc.3413 .

Abatzoglou, J.T., E. Fleishman, E.L. Williams, D.E. Rupp, J.S. Jenkins, and M. Sadegh. 2024. The efficacy of red flag warnings in mitigating human-caused wildfires across the western united states. *J. Appl. Meteor. Climatol.* 63: 1511–1521. https://doi.org/https://doi.org/10.1175/JAMC-D-24-0120.1 .

Ahmadov, R., G. Grell, E. James, I. Csiszar, M. Tsidulko, B. Pierce, S. McKeen, S. Benjamin, C. Alexander, G. Pereira, S. Freitas, and M. Goldberg 2017. Using viirs fire radiative power data to simulate biomass burning emissions, plume rise and smoke transport in a real-time air quality modeling system. In *2017 IEEE International Geoscience and Remote Sensing Symposium (IGARSS)*, pp. 2806–2808.

Al-Yaari, A., T. Condom, C. Junquas, A. Rabatel, V. Ramseyer, J.E. Sicart, M. Masiokas, S. Cauvy-Fraunié, and O. Dangles. 2023. Climate variability and glacier evolution at selected sites across the world: Past trends and future projections. *Earth's Future 11*(10): e2023EF003618. https://doi.org/https://doi.org/10.1029/2023EF003618 .

Balch, J.K., V. Iglesias, A.L. Mahood, M.C. Cook, C. Amaral, A. DeCastro, S. Leyk, T.L. McIntosh, R.C. Nagy, L.S. Denis, T. Tuff, E. Verleye, A.P. Williams, and C.A. Kolden. 2024. The fastest-growing and most destructive fires in the US (2001 to 2020). *Science 386*(6720): 425–431. https://doi.org/10.1126/science.adk5737. https://www.science.org/doi/pdf/10.1126/science.adk5737 .

California Annual Operating Plan. 2025. California Annual Operating Plan 2025. https://www.weather.gov/media/wrh/cafw/2025_CA_FIRE_AOP.pdf.

Carney, M. 2026, June. Full account of highway 82 fire: Historic destruction, massive response detailed by state officials. *WTOC 11* .

Cayan, D.R., L.L. DeHaan, A. Gershunov, J. Guzman-Morales, J.E. Keeley, J. Mumford, and A.D. Syphard. 2022, 10. Autumn precipitation: the competition with Santa Ana winds in determining fire outcomes in southern California. *International Journal of Wildland Fire 31*(11): 1056–1067. https://doi.org/10.1071/WF22065 .

D'Evelyn, S.M., L.M. Wood, C. Desautel, N.A. Errett, K. Ray, J.T. Spector, and E. Alvarado. 2023. Learning to live with smoke: characterizing wildland fire and prescribed fire smoke risk communication in rural washington. *Environmental Research: Health 1*(2): 025012. https://doi.org/https://doi.org/10.1088/2752-5309/acdbe3 .

Edgeley, C.M. and J.T. Burnett. 2025, 01. Understanding rural adaptation to smoke from wildfires and forest management: insights for aligning approaches with community contexts. *International Journal of Wildland Fire 34*(1): WF24016. https://doi.org/10.1071/WF24016. https://connectsci.au/wf/article-pdf/doi/10.1071/WF24016/1636671/wf24016.pdf .

Giglio, L., T. Loboda, D.P. Roy, B. Quayle, and C.O. Justice. 2009. An active-fire based burned area mapping algorithm for the modis sensor. *Remote Sensing of Environment 113*(2): 408–420. https://doi.org/https://doi.org/10.1016/j.rse.2008.10.006 .

Giglio, L., W. Schroeder, and C.O. Justice. 2016. The collection 6 modis active fire detection algorithm and fire products. *Remote Sensing of Environment* 178: 31–41. https://doi.org/https://doi.org/10.1016/j.rse.2016.02.054 .

Guirguis, K., B. Hatchett, R. Clemesha, R. Aguilera, A. Gershunov, I. Campbell, D. Cayan, and M. Merrifield. 2025, Dec. Compound atmospheric drivers of the catastrophic 2025 Los Angeles urban firestorm. *npj Natural Hazards 2*(1): 103. https://doi.org/10.1038/s44304-025-00155-7 .

Hantson, S., N. Andela, M.L. Goulden, and J.T. Randerson. 2022, May. Human-ignited fires result in more extreme fire behavior and ecosystem impacts. *Nature Communications 13*(1): 2717. https://doi.org/10.1038/s41467-022-30030-2 .

Hatchett, B.J., C.M. Smith, N.J. Nauslar, and M.L. Kaplan. 2018. Brief Communication: Synoptic-scale differences between Sundowner and Santa Ana wind regimes in the Santa Ynez Mountains, California. *Natural Hazards and Earth System Sciences 18*(2): 419–427. https://doi.org/10.5194/nhess-18-419-2018 .

Hatchett, B.J. and E.M. Wells. 2026. Good fire weather. *Bulletin of the American Meteorological Society* 107: E1323–E1334. https://doi.org/https://doi.org/10.1175/BAMS-D-25-0209.1 .

Hesseln, H. 2018, Dec. Wildland fire prevention: a review. *Current Forestry Reports 4*(4): 178–190. https://doi.org/10.1007/s40725-018-0083-6 .

Hoekstra, S., J. Vickery, and B.J. Hatchett. 2026. Igniting insight: Evaluating nws red flag warnings within a fire partner decision-making context. *Bulletin of the American Meteorological Society 107*(4): E884 – E901. https://doi.org/10.1175/BAMS-D-25-0036.1 .

Keeley, J.E. and A.D. Syphard. 2019, Jul. Twenty-first century california, usa, wildfires: fuel-dominated vs. wind-dominated fires. *Fire Ecology 15*(1): 24. https://doi.org/10.1186/s42408-019-0041-0 .

Lasantha, V., T. Oki, and D. Tokuda. 2022. Data-Driven versus Köppen–Geiger systems of climate classification. *Advances in Meteorology 2022*(1): 3581299. https://doi.org/https://doi.org/10.1155/2022/3581299 .

Omernik, J.M. and G.E. Griffith. 2014, Dec. Ecoregions of the conterminous United States: evolution of a hierarchical spatial framework. *Environmental Management 54*(6): 1249–1266. https://doi.org/10.1007/s00267-014-0364-1 .

Orland, E., T.D. McCabe, Y. Chen, R.C. Scholten, Z. Becker, R.A. Loehman, J.T. Randerson, S.R. Coffield, T. Liu, A.N. Shiklomanov, K. Nelson, B. Peterson, M.B. Follette-Cook, and D.C. Morton. 2025, Oct. Near real-time indicators of burn severity in the western U.S. from active fire tracking. *Fire Ecology 21*(1): 55. https://doi.org/10.1186/s42408-025-00407-x .

Sablan, O., B. Ford, E. Gargulinski, M.S. Hammer, G. Henery, S. Kondragunta, R.V. Martin, Z. Rosen, K. Slater, A. van Donkelaar, H. Zhang, A.J. Soja, S. Magzamen, J.R. Pierce, and E.V. Fischer. 2024. Quantifying prescribed-fire smoke exposure using low-cost sensors and satellites: Springtime burning in eastern kansas. *GeoHealth 8*(4): e2023GH000982. https://doi.org/https://doi.org/10.1029/2023GH000982 .

Schlobohm, P. 2000. Application of the fire danger pocket card for firefighter safety. https://wildfireweb-prod-media-bucket.s3.us-gov-west-1.amazonaws.com/s3fs-public/2022-11/pc_apply.pdf.

Short, K.C., I.C. Grenfell, K.L. Riley, and K.C. Vogler. 2020. Pyromes of the conterminous United States. Fort Collins, CO: Forest Service Research Data Archive.

Snethlage, M., J. Geschke, E. Spehn, A. Ranipeta, N. Yoccoz, C. Körner, W. Jetz, M. Fischer, and D. Urbach. 2022. GMBA Mountain Inventory v2.

Snethlage, M.A., J. Geschke, A. Ranipeta, W. Jetz, N.G. Yoccoz, C. Körner, E.M. Spehn, M. Fischer, and D. Urbach. 2022, Apr. A hierarchical inventory of the world's mountains for global comparative mountain science. *Scientific Data 9*(1): 149. https://doi.org/10.1038/s41597-022-01256-y .

Svoboda, M., D. LeComte, M. Hayes, R. Heim, K. Gleason, J. Angel, B. Rippey, R. Tinker, M. Palecki, D. Stooksbury, et al. 2002. The drought monitor. *Bulletin of the American Meteorological Society 83*(8): 1181–1190 .

Sweeney, B., W.M. Jolly, P.H. Freeborn, and C. Ochocki. 2025. ClassiFiRxe: a data-driven tool to support prescribed fire planning and implementation. *Preprint submitted to SSRN*. https://doi.org/http://dx.doi.org/10.2139/ssrn.5846214 .

Swetnam, T.W., D.A. Falk, E.K. Sutherland, P.M. Brown, and T.J. Brown. 2011. Final report, 2011: Fire and climate synthesis (facs) project, jfsp 09-2-01-10. https://www.researchgate.net/publication/292610619_Final_Report_2011_Fire_and_Climate_Synthesis_FACS_Project_JFSP_09-2-01-10.

The MathWorks Inc. 2024. Matlab version: 24.1.0 (r2024a).

Worsnop, R.P., A. Hoell, B.J. Hatchett, T.B. Chapman, M.L. Breeden, Z. Zach Tolby, K.C. Short, and M. Hobbins. 2026. Characterizing windows of opportunity for prescribed pile and broadcast burning in Northern California. *Fire Ecology* 22. https://doi.org/10.1186/s42408-026-00492-6 .